Measurements of Anisotropic Temperatures in Magnetized Gas-Jet Plasmas

Z. BARFIELD, J. L. PEEBLES, P. TZEFERACOS, D. MASTROSIMONE, J. KATZ, P. V. HEUER, and D. H. FROULA

University of Rochester, Laboratory for Laser Energetics

Introduction

- Magnetized plasma experiments are becoming increasingly frequent as we develop new ways to generate stronger external fields
  - magnetized flows for high-energy-density physics (HEDP) and laboratory astrophysics at MAGPIE [1]
  - magnetized liner inertial fusion (MagLIF) experiments on Z [2], and mini-MagLIF on OMEGA [3]
- In the presence of a magnetic field, electron thermal transport is suppressed [4]. This is a desirable effect when heat confinement is the goal of an experiment.
- The experiment discussed in this work shows that a magnetic field can also affect the microscopic scale under certain conditions, creating anisotropic electron temperatures
  - these conditions are similar to the preheat plasma in some MagLIF experiments; the experimental results could provide useful benchmarks for the models used to predict MagLIF preheat

E30366

Experimental Details

- This experiment used a Mach-5 supersonic gas-jet nozzle with an exit diameter of 2 mm. The experiment and measurements took place 2 mm above the nozzle exit. The pressures used produced a nitrogen gas with molecular densities ranging from 6×10^{17} cm^{-3} to 1.4×10^{18} cm^{-3} resulting in electron densities between 3 to 7×10^{18} cm^{-3}
- A Dual-MIFEDS* unit produced a 15 T magnetic field which was uniform throughout the region of interest
- 100-J, 500-ps 3ω beams preheated the plasma. A 2-ns, 80-J 2ω beam was used at the main drive along the axis of the magnetic field, as well as a Thomson-scattering beam. Alternating two different 2-ns, 20-J 3ω Thomson beams resolved the plasma conditions parallel and perpendicular to the magnetic field.

E30367

*MIFEDS: magneto-inertial fusion electrical discharge system

Diagram

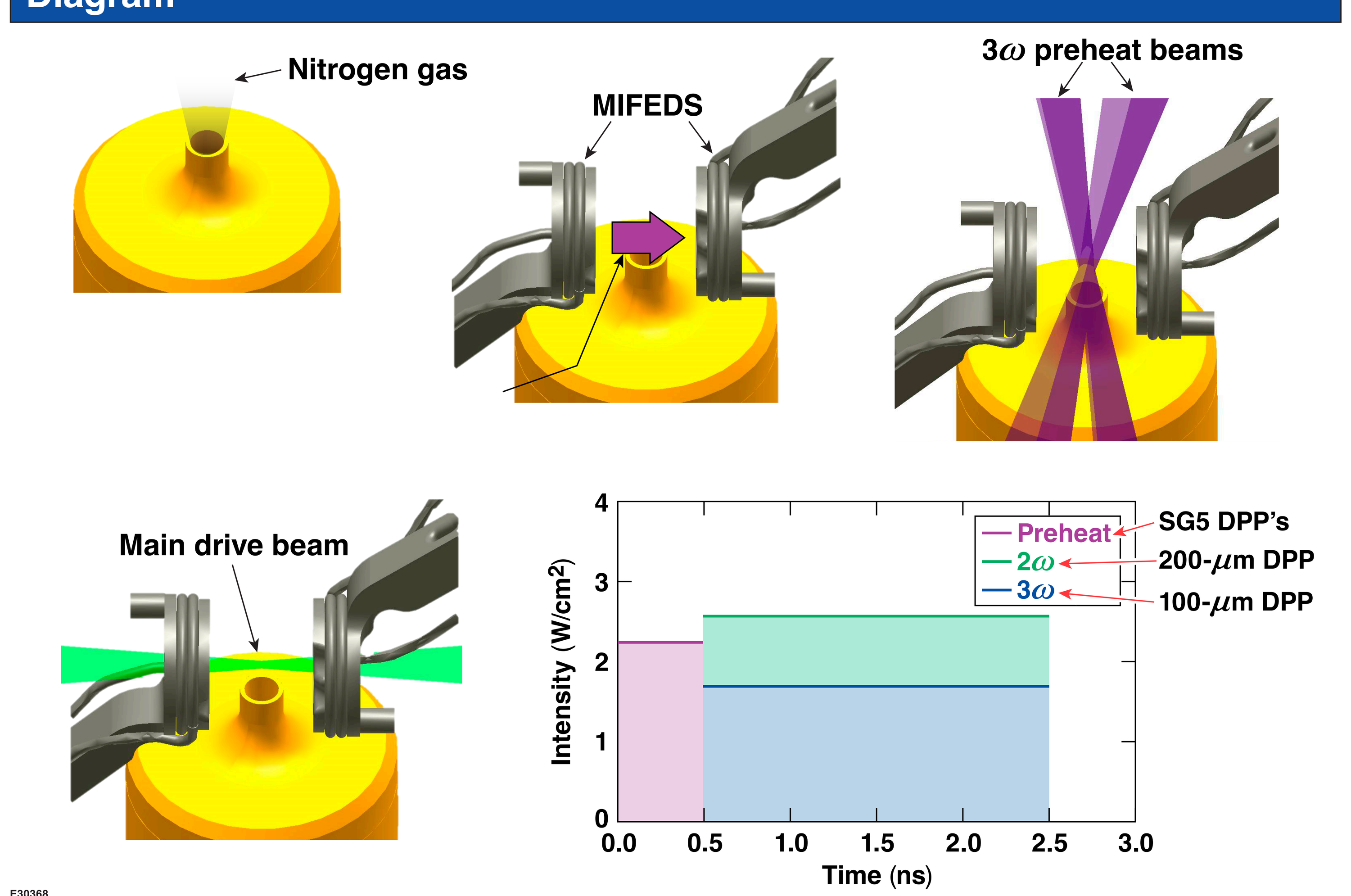

E30368

Thomson-Scattering Geometry

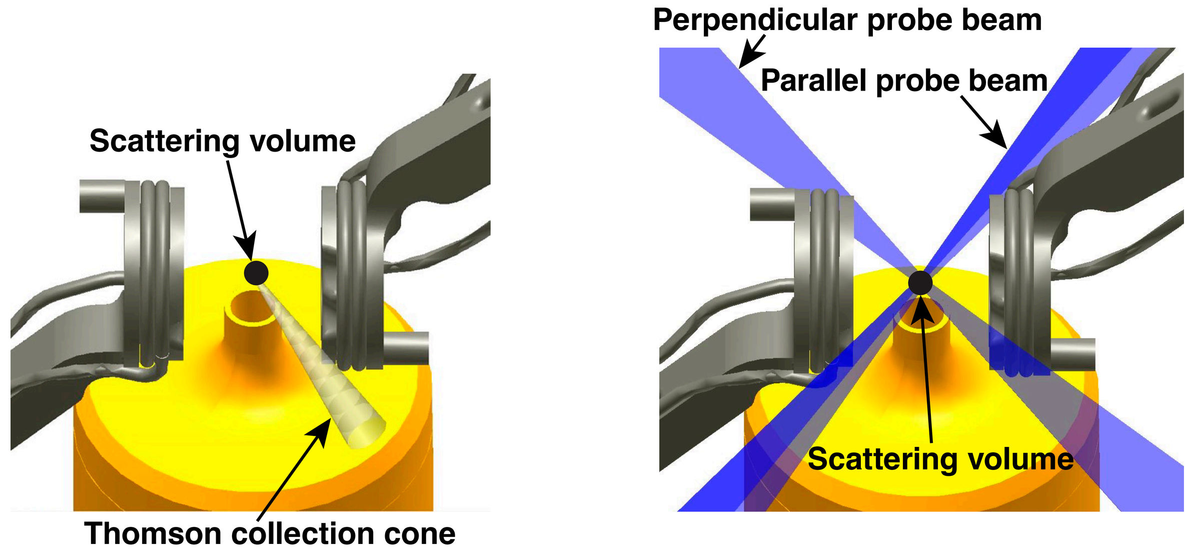

E30369

Anisotropic Electron Temperatures

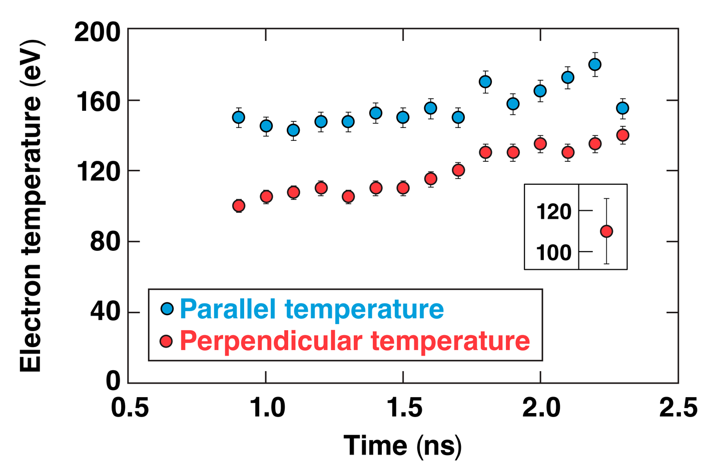

Electron temperatures are measured from low-frequency ion-acoustic fluctuations using a 3ω Thomson probe. The relative error between the temperatures in the parallel and perpendicular direction is less than 5%. Absolute error from the assumptions in the fitting model is 14.5% (shown in inset.)

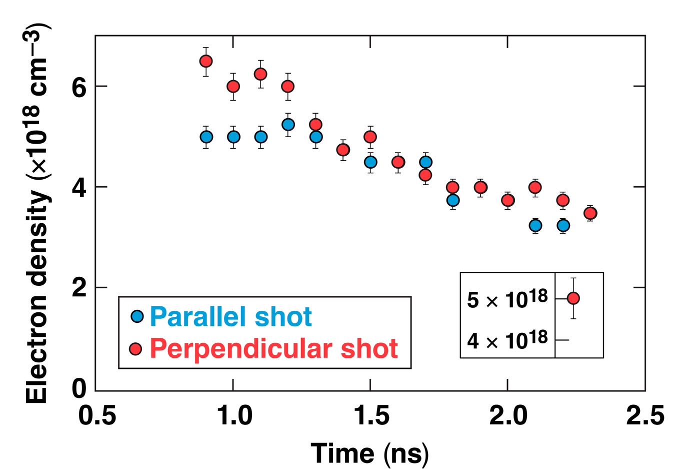

Electron densities measured from high-frequency electron plasma fluctuations using a 2ω Thomson probe (co-timed with the 3ω probe). The relative error between the two data sets is less than 5%. Absolute error from the assumptions in the fitting model is 9.7% (shown in inset.)

E30370

Analysis of Results

Lineouts at 1.5 ns for a pair of low-density shots

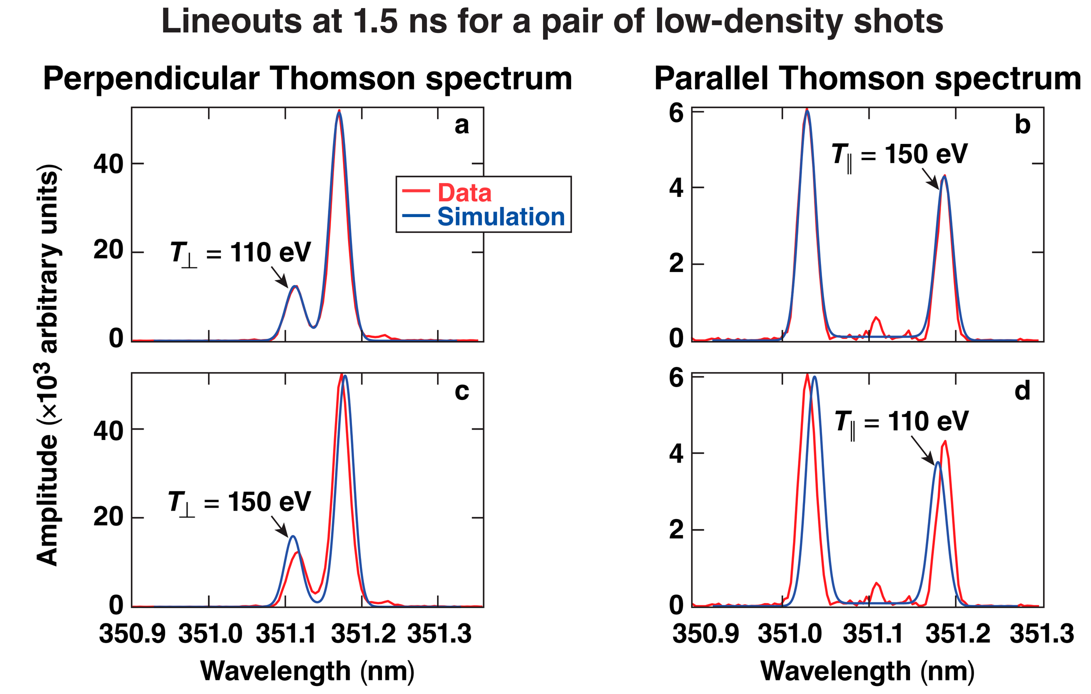

Figures a and b show the simulation fits (blue) to the experimental Thomson spectra (red). These are fit with perpendicular and parallel temperatures $T_\perp$ = 110 eV and $T_\parallel$ = 150 eV.

The lower figures, c and d, show the same experimental Thomson spectra (red), but with simulation spectra (blue) produced using the fit temperature from the *opposite* spectrum. These fits demonstrate that the relative error in the temperature measurements are much smaller than the observed temperature discrepancy. The relative error is 3.7% compared to a temperature discrepancy between 27% and 36%.

E30375

Fitting Details

- The non-Maxwellian order of the electron distribution was assumed to be $m = 3$ [6, 7] and the ionization state of the nitrogen was assumed to be $Z = 5$
- The form factor of the scattered light is determined by the1-D projection of the particle velocity distribution functions (VDF's), f_{eo} and f_{io} [7]

$$S(\vec{k}, \omega) = \frac{2\pi}{k}\left|1-\frac{\chi_e}{\epsilon}\right|^2 f_{eo}\left(\frac{\omega}{k}\right) + \frac{2\pi Z}{k}\left|\frac{\chi_e}{\epsilon}\right|^2 f_{io}\left(\frac{\omega}{k}\right)$$

- The geometry of the Thomson-scattering beams was chosen such that the 1-D VDF's were either parallel or perpendicular to the external magnetic field
- Density gradients of ±10% to 20% are observed within the scattering volume (~100 μm^3) of the high-frequency, electron plasma wave feature. These are believed to be due to the evolution of the density profile within the magnetic field and are consistent with previous results from this platform

E30371

Generation of Anisotropy

- The anisotropy is present while the main drive beam is on; it is therefore believed that advection of the magnetic field from the scattering volume is causing the perpendicular temperature to decrease at a rate comparable to the collision time.
- Double-adiabatic theory suggests the perpendicular temperature decreases linearly with the magnetic field [8]
  - if the magnetic field is being advected fast enough, there could be a dynamic balance between adiabatic expansion (generating the anisotropy) and electron collisions (working to isotropize the distribution)

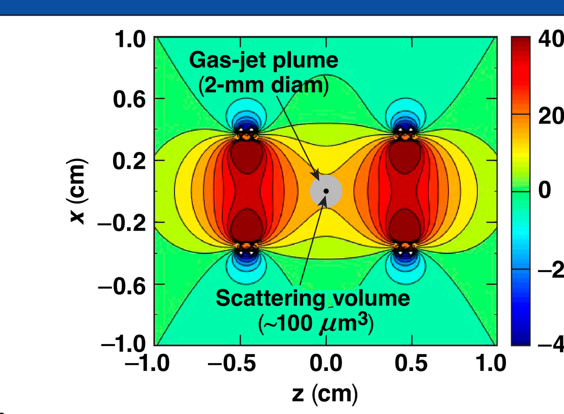

- Electron–ion collision time: τ_{ei} = 3 ps, Hall parameter: $\omega_{ce}\tau_{ei} = \frac{\lambda_{ei}}{r_{Le}} = 7$, Collision scale: $k\lambda_{ei} = 10$
- The macroscopic field profile outside of the scattering volume is shown here

E30372

Future Work

- The next experiment on this platform will utilize monoenergetic protons to image the magnetic-field profile in the plasma. Multiple techniques, including the addition of a high-*Z* mesh [9,10] will be used to minimize the error on a measurement of the field strength within the scattering volume.
- The images below are from proton deflectometry simulations performed in *PlasmaPy* [11]. The protons are deflected through the vacuum magnetic field produced my MIFEDS (plot above) and collected onto a synthetic CR-39 detector 27 cm away and binned with 400-μm resolution (magnification = 28)
- The right-hand plot has the magnetic-field perturbation from a *HYDRA* simulation [12] superimposed onto the MIFEDS field. The magnetic field is driven out of the center of the plasma by the temperature gradients from the 2ω main-drive beam. This effect is noticeable as the change in the shape of the image near the top edge of the CR-39.

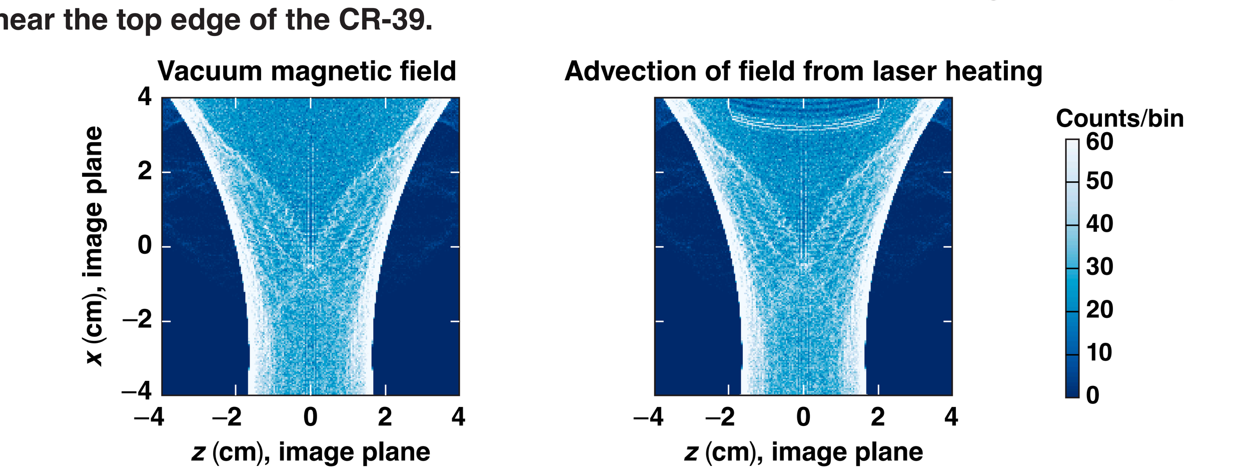

E30368

References

[1] G. F. Swadling *et al.*, Rev. Sci. Instrum. 85, 11E502 (2014).
[2] S. A. Slutz *et al.*, Phys. Plasmas 17, 056303 (2010).
[3] D. H. Barnak *et al.*, Phys. Plasmas 24, 056310 (2017).
[4] S. I. Braginskii, in Reviews of Plasma Physics, edited by M. A. Leontovich (Consultants Bureau, New York, 1965), Vol. 1, p. 205.
[5] A. B. Langdon, Phys. Rev. Lett. 44, 575 (1980).
[6] J. P. Matte *et al.*, Plasma Phys. Control. Fusion 30, 1665 (1988).
[7] D. H. Froula *et al.*, Plasma Scattering of Electromagnetic Radiation: Theory and Measurement Techniques, 2nd ed. (Academic Press, Amsterdam, 2011).
[8] G. F. Chew *et al.*, Proc. R. Soc. A: Math. Phys. Eng. Sci. 236, 112 (1956).
[9] C. L. Johnson *et al.*, Rev. Sci. Instrum. 93, 023502 (2022).
[10] S. Malko *et al.*, Appl. Opt. 61, C133 (2022).
[11] PlasmaPy Community *et al.*, PlasmaPy (version 0.0.7), Zenodo, Accessed 27 May 2022, https://doi.org/10.5281/zenodo.4037407
[12] L. Leal, Laboratory for Laser Energetics, private communication (2022).

E30374

UNIVERSITY of ROCHESTER